

Combined Rule-Based and Generative Artificial Intelligence in the Design of Smartphone Optics

NENAD ZORIC^{1,*}, SIMON THIBAUT², MARIE-ANNE BURCKLEN³, LIJO THOMAS^{2,4},
MOMCILO KRUNIC^{1,5}, YUNFENG NIE⁶

¹Faculty of Technical Sciences, University of Novi Sad, 21000 Novi Sad, Serbia

²Centre d'Optique, Photonique et Laser, Université Laval, G1V 0A6 Québec, Canada

³Institut d'Optique Graduate School, University Paris-Saclay, Paris, France

⁴L3Harris Technologies Inc., L4K-M9W, Toronto, Canada

⁵Labsoft AI, The Science and Technology Park, 21102, Novi Sad, Serbia

⁶Department of Applied Physics and Photonics, Vrije Universiteit Brussel, B-1050 Brussels, Belgium

*Corresponding author: zoric.de17.2019@uns.ac.rs

Received XX Month XXXX; revised XX Month, XXXX; accepted XX Month XXXX; posted XX Month XXXX (Doc. ID XXXXX); published XX Month XXXX

Abstract: This paper reports on a study of design methodology for smartphone lenses utilizing generative and rule-based artificial intelligence (AI) algorithms. The proposed innovative design method utilize the GPT-4, an OpenAI model to generate macros for global optimization algorithms used in designing smartphone lenses. A comprehensive global search for optimal starting points of smartphone lenses has been conducted to obtain training sets. We trained GPT-4 model developing framework for coding of macros, creation of merit function and evaluation of obtained starting designs. The results demonstrate the practical value of the proposed design methodology based on AI algorithms in the design of a 21.4 megapixel smartphone lens.

1. INTRODUCTION

We are witnessing and living in an era where machine intelligence is beginning to influence most domains of science and engineering.

In 1956, John McCarthy introduced the term AI to describe machines like the “Logic Theorist” that could reason. According to Wang [1], AI refers to information processing systems that adapt to their environment using available resources and knowledge. Currently, the intelligence quotient (IQ) of artificial intelligence ranges from 100 to 120, which indicates that it is already more capable and efficient than most of the average humans in solving and performing specific tasks. Predictions suggest that very likely, AI could soon achieve an IQ in the range of several thousand.

The remarkable capabilities of this new form of intelligence in our world have already provoked significant skepticism and fear across various professional domains. One group, including designers, programmers, and engineers, seeks to embrace and synergize their expertise with these advanced algorithms. Meanwhile, others view these developments with skepticism and warn of the potential consequences AI may have on the formation of future civilization and economy.

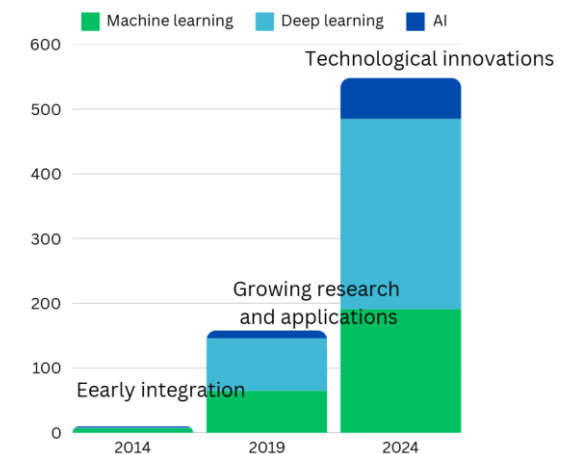


Fig. 1. Increasing trend of research topics on the application of artificial intelligence in the field of optical engineering.

The authors of this study believe that the synergy between human effort and artificial intelligence, through their complementary contributions, represents a very effective approach for achieving reliable and high-quality results in optical design. Traditional optical design relies heavily on iterative methods led by experienced designers, often demanding extensive computational resources and domain-specific expertise.

In the last decade, we have witnessed significant advancements in the application of AI in optics and photonics, evolving from conceptual research to practical implementation. Three key stages can be observed throughout this period. The first stage marks the early research and integration, where researchers began implementing artificial intelligence into optical networks, offering more efficient solutions. From 2018 to 2022, there was a rapid surge in various fields of photonics, driven by machine and deep learning solutions [2, 3]. Fig. 1 shows statistics based on papers published in *Applied Optics* and *Optics Express* with the keywords: artificial intelligence, machine learning, and deep learning. Since 2022, the impact of AI on optics and photonics has become even more pronounced, leading to major technological innovations.

In 2024, John Hopfield and Geoffrey Hinton were awarded the Nobel Prize in Physics for their pioneering work on artificial neural networks. In the same year, the XLuminA software was introduced in super-resolution microscopy, accelerating innovations based on AI in the field of optics [4].

This study investigates an innovative approach to smartphone lens design, leveraging generative AI to produce macros of global search algorithm, and merit function and evaluate starting design. Generative AI models, such as ChatGPT, have demonstrated an amazing ability to generate scripts and code that guide optimization algorithms toward effective solutions. ChatGPT is based on the neural network using billions of parameters [5].

In scenarios requiring a blend of creativity, visualization, logical reasoning, and responsiveness to real-time needs, AI-driven design solutions remain at the threshold of efficiency and clarity. To illustrate the experience of designers in the sneaker industry utilizing AI-based application “Imagine an army of little aliens attempting to draw shoes. They might be fantastic at it, but they lack the earthly wisdom of what a shoe truly entails. AI-based applications, like ChatGPT and Midjourney, are still in their infancy and don’t quite grasp the intricate details of shoe construction [6].”

Despite the well-known challenges of generative AI, such as errors or hallucinations, an expert from shoe industry expressed optimism, describing AI as rocket fuel for creativity. They emphasized that AI is not a replacement for human creativity but an amplifier, calling it “an amazing tool guided by human imagination [7].”

Our experience in training OpenAI model has shown that optical designers can rely on the code and formulas generated by the AI large language model (LLM) with a high degree of accuracy. Currently, deep learning methods can directly generate initial configurations, including approaches based on supervised learning [8, 9], unsupervised learning [10], and end-to-end models [11]. Although current applications are generally limited to single structures, introducing dynamic networks holds substantial potential for solving a broader range of optical configurations.

Dilworth, by incorporating an artificial intelligence (AI) feature into his optical lens design software, SYNOPSIS OSD, demonstrated remarkable foresight in recognizing the potential of machine

intelligence nearly 40 years ago. The rule-based AI algorithms within the software could perform complex tasks related to the evaluation and optimization of optical systems, relying on only a few textual commands [12].

The application of AI into optical design has been explored in previous works [13], where rule-based AI [14], and deep-learning models support the generation of starting designs.

Recently, Yang et al. developed a framework based on deep learning that uses a step-by-step approach to create lens designs from scratch, eliminating the need for a starting design. This method can automatically design both standard and advanced lenses, such as those used in cellphones, making them compact and highly efficient [15].

The novelty of our study lies in its application of generative AI as an active contributor to the design process through the creation of macros and evaluation of starting designs, enabling the automation of global search optimization. Additionally, this generative approach adds value by reducing the time required to generate merit function macros with optimized aspheric surfaces for smartphone lenses. By focusing on a rule-based AI algorithms for automatic aspherical assignment and automatic glass replacement, the proposed design approach achieves a higher level of automated lens design.

In that sense, the conducted study lays the foundation for future advancements in AI applications, ultimately pushing the boundaries of what is achievable in future of lens design.

The remainder of this paper is structured as follows. Section 2 explains the training of the GPT-4 model for writing macros, as well as the search for the best methodology for generating the initial design of smartphone lens. Section 3 addresses the optimization process of the initial design using rule-based AI algorithms for adding aspheric surfaces and additional refractive elements. Section 4 concludes with a discussion of the proposed methodologies and the advantages brought by the application of AI in optical design.

2. SUPERVISED TRAINING OF GENERATIVE AI ON DESIGN SEARCH

The evolution of smartphone optics is driven by the increasing demand for advanced mobile photography, with users seeking professional-quality imaging in compact devices.

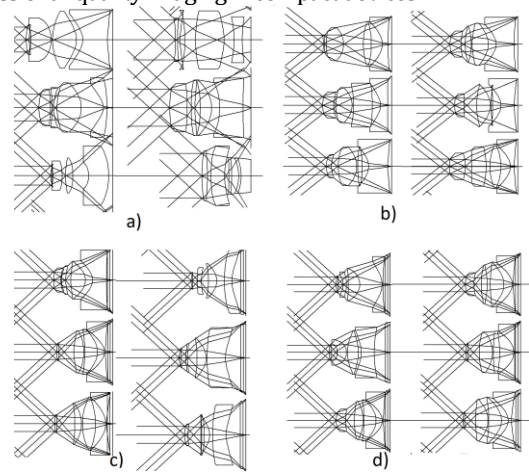


Fig. 2. Starting designs of smartphone lens for (a) 16 megapixels camera, generated with weak weights of distortion control (b) 16 megapixels camera, generated with strong weights of distortion constraints (c) 21.4 megapixels camera, generated with weak weights of distortion control (d) 21.4 megapixels camera, generated with strong weights of distortion constraints

megapixel camera, generated with illumination control in 5 field points (d)
21.4 megapixel camera, generated with illumination control in three field points.

High-resolution sensors, paired with advancements in computational imaging, have become a cornerstone of the most widely accepted smartphones [16]. Emerging trends, including the integration of aspheric lenses, free-form lenses, and hybrid materials like glass-polymers, are further transforming smartphone optics, offering new opportunities to push the boundaries of mobile imaging [17,18]. Since the invention of CCD (Charge-Coupled Device) technology, digital photography has been revolutionizing the world, ushering in an era where images are increasingly replacing words [19]. Integrating CCD sensors into smartphones is challenging due to their higher power consumption and larger size, which is why CMOS sensors are more commonly used.

To define the image specifications, we selected the Omnivision® OV21840 CMOS image sensor, which features an active array of 5344 x 4016 pixels, providing a resolution of 21.4 megapixels.

The diagonal of the sensor is 7.90 mm with pixel size of 1.12 micrometers. The image height is defined as half of the sensor's diagonal, yielding ≈ 3.953 mm. To mitigate the risk of image vignetting and ensure optimal image quality on the sensor array, the image height is set to 3.99 mm, slightly exceeding the required value. Optical characteristics of smartphone lens are presented in table 1.

Table1. Optical characteristics of smartphone lens

Wavelengths	486 nm -656 nm
Field number, FN	2.5
Semi field of view, FOV/2	41.5 °
Entrance pupil semi aperture	0.9 mm
Image height	3.99 mm
Focal length	4.5 mm
Front working distance	infinite
Back focal distance	3 mm

Current applications of artificial intelligence in optics are generally restricted to specific optical structures, due to the numerous variables at play. In this design strategy, we utilize an OpenAI model to overcome the challenges of the design tasks that were previously addressed manually and analytically in our studies, which were based on global optimization strategies.

In principle, we transfer the task of writing and editing macros (global search and merit function) to an OpenAI model, giving it feedback about successful outputs.

To find an efficient strategy for smartphone camera design, we started with a design resolution of 16 megapixels and progressed to a design with 21.4 megapixels, increasing the semi FOV from 38° to 41.5°.

The main idea is to obtain a useful starting design using a global search algorithm (Design Search) in Synopsys OSD, and then train an OpenAI model with macros that were successful in exploring starting designs.

As we progressed with the generated starting designs of the Design search, we trained a GPT-4 model using macros that yielded the best results, along with an explanation of the types of operands and constraints used to control optical aberrations, distortions, and illumination. OpenAI model, the GPT-4 can process

textual requests, analyze images, and read text from images. In addition, we trained a GPT-4 on the basic equations of applied optics related to F-number (FN), entrance pupil diameter (DN), field of view (FOV), focal length, and image height. The pre-training involves copying text and equations, supplemented with additional information derived from textual comments within the GPT-4 module.

We began with a smaller FOV of 76 degrees so that the image height was lower, suitable for a 16-megapixel camera. Design goals are the transverse aberrations' maximum of 0.05 mm, with no ray tracing errors and a lens arrangement of convex, concave, and convex-concave lenses. Fig. 2 shows the initial designs using different macros as we explored the best approach.

In the first phase, we used a design approach using monitors for distortion in the macros and requests for two plastic materials. However, obtained starting points implied that weak weights of monitors for distortion caused significant ray tracing errors in Fig. 2 (a) [20]. To overcome this issue, monitor weights were increased in macros. In addition, we decreased the number of monitors from six to three field points. Such a macro has generated starting points, shown in Fig. 2 (b).

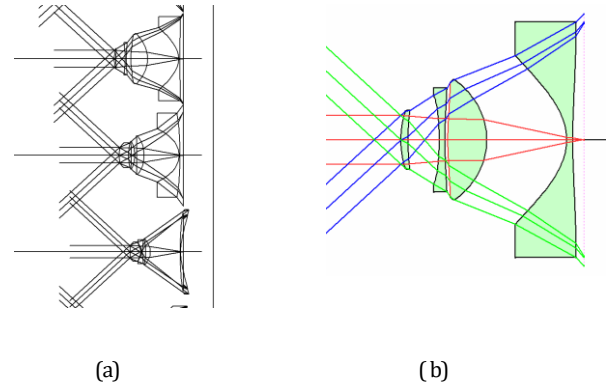


Fig. 3. Starting design of smartphone lens for 21.4 megapixel (a) three outputs of global search algorithm (b) selected for further optimization.

In the next trial, the monitors for distortion control were replaced with monitors for illumination, ensuring that illumination gradually decreased toward the field edges. Further, we added a request for a cover glass in macros and increased semi-field to 41.5 degrees. The cover glass protects the sensor and provides additional achromatization. We constrained the illumination to 38% at the edge of the field, with the intention of increasing it during optimization. With well-adjusted monitor weights, the obtained starting designs in Fig 2. d) showed good performance, including proper lens arrangements, accurate ray tracing, and transverse aberrations of 0.05 mm or less. The global search algorithm explored solutions based on macro parameters, finding designs that involved three aspheric coefficients for all lens surfaces, the conic constant, and higher-order even aspheres (third and sixth orders). The task was performed using two plastic materials (OKP4 and ZEON480R). The implemented macros for the global search were effective in generating designs with a satisfactory design and promising image quality.

In Fig. 3a), three starting designs from one global search run are shown. In this run, we obtained designs with relative illumination exceeding 40% and transverse aberrations corrected to 0.05 mm.

We selected a starting point in Fig. 3 b), which had lens arrangement of convex, concave, and convex-concave lenses.

Fig. 4 illustrates the imaging quality for the central field and RMS spot size over field [21]. Imaging quality analysis of photography was performed using image tools in Synopsys OSD (colorized photography of scientist and inventor Nikola Tesla).

To simulate the image quality of a part of a photograph, it is necessary to increase the number of color wavelengths. In this simulation, we obtained a realistic color balance with 7 color wavelengths in the visible spectrum.

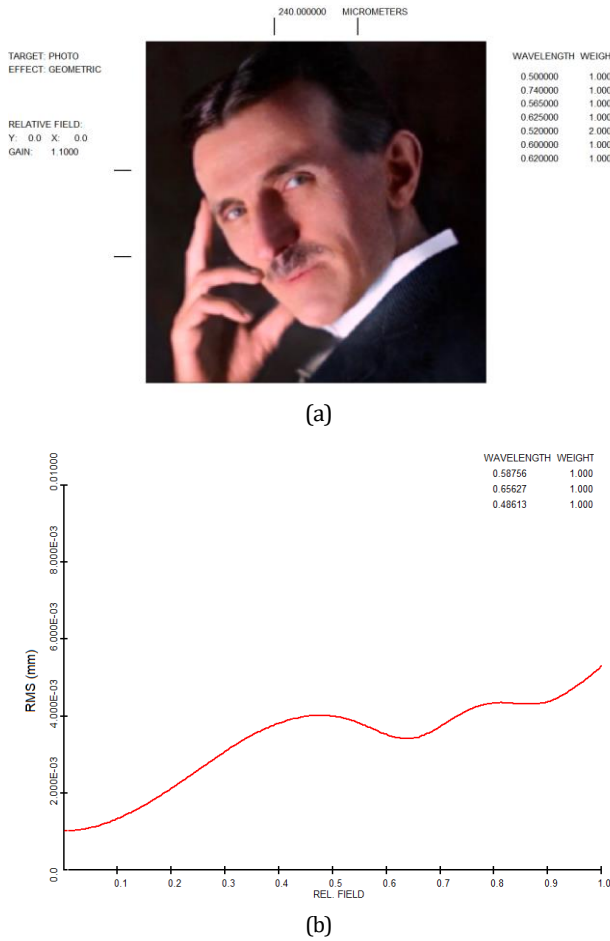


Fig. 4. Starting design assessment: (a) imaging quality analysis of photography on central field (b) RMS spot size over field.

$$\text{Dairy} = 2.44\lambda \times \text{FN} = 3.7 \text{ micrometers} \quad (1)$$

Based on the airy disk criterion, the RMS spot radius should be less than 3.7 micrometers over the entire field of view. Given a pixel size of 1.12 micrometers for a 16-megapixel sensor, and considering that the ideal RMS spot radius should not exceed 2 pixels, we set a target of 2.24 micrometers for the simulated pixel size. The simulation visualizes a region of image covering a width of 960 micrometers, while the total sensor width is 6.4 mm.

As expected for wide-angle lenses, optical aberrations are much more noticeable at the edges of the field. The simulation does not include distortion, which is about 4% at the edge of the field of

view (FOV). Macro 1 (see Supplement 1) was used to train the GPT-4 model for design strategy with assigned plastic materials.

To explore more possibilities for starting designs, we also tried the second design approach, where we included a glass model and protective cover glass in the global search algorithm. By allowing the algorithm to explore solutions with glass models, we may gain better and new shapes of starting designs [22].

Macro 2, written by the GPT-4 (see Supplement 1) was successful after adjusting (fine-tuning model) the monitors for illumination at three field points. It should be emphasized that illumination and distortion are conflicting constraints, and it is necessary to find a balance in the requirements for image quality.

As shown in Fig. 5 we obtained different starting designs with transversal aberration in range of 0.02 to 0.05 mm.

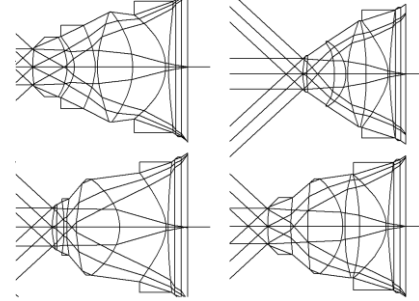


Fig. 5. Starting designs of smartphone lens for 21.4 megapixel with glass model and cover glass.

In this design task, the global search algorithm is entrusted with identifying the starting design that achieves minimal transverse aberrations. Design Search has selected upper left design in Fig. 5 as the best choice with minimal transverse aberration. Regarding the Modulation Transfer Function (MTF) of smartphone lens, criteria is associated with the Nyquist frequency of the sensor. Given the sensor's pixel size of 1.12 μm , the system's maximum spatial resolution can be determined as:

$$V_{\text{Nyquist}} = 1 / 2 \times \text{CMOS pixel size} = 446.4 \text{ lp/mm} \quad (2)$$

The multifield MTF shown in **Fig. 6** illustrates that the central field and half of the field of view are already within the limits that meet the image resolution requirements. The MTF of the central field is greater than 0.5 at half of the maximum spatial frequency of 223 lp/mm.

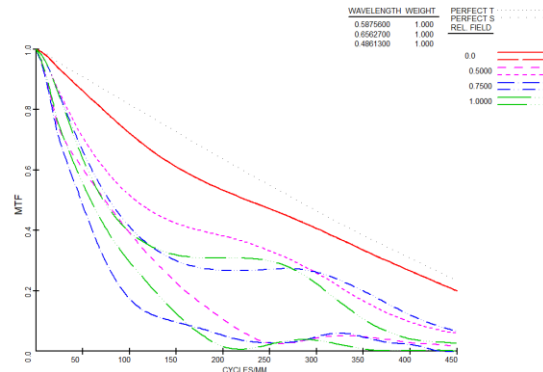


Fig. 6. Multifield modulation transfer function of starting design.

Fig 7. presents imaging quality analysis of selected starting design (upper left) from Fig. 5.

As shown in Fig. 7 (a), starting design already exhibited good image quality of photography in central FOV (colorized photography of s physicists George Smith and Willard Boyle-inventors of CCD technology). This result indicates the remarkable capabilities of the global search algorithm when the requests and operands are set properly.

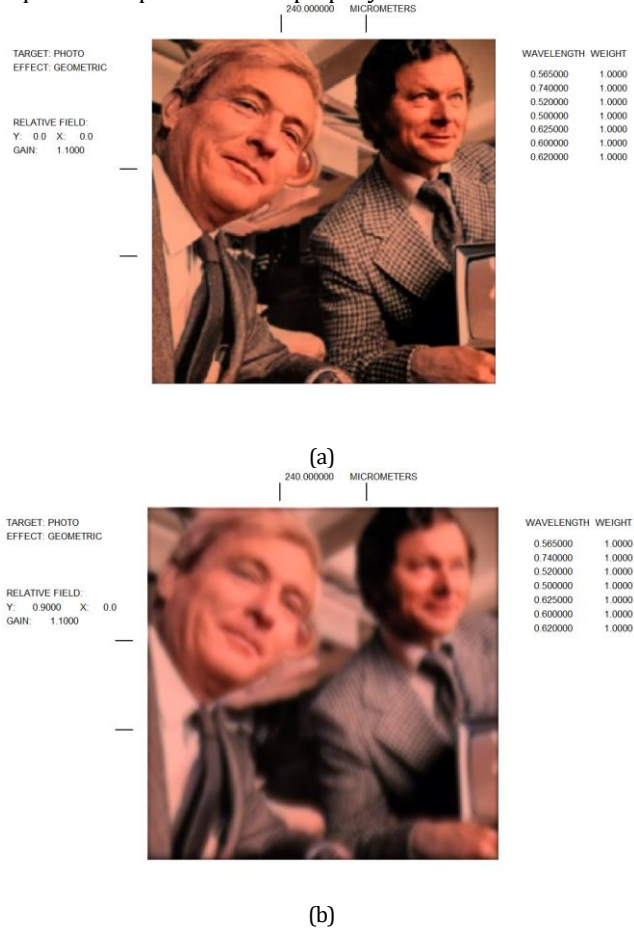


Fig. 7. Imaging quality analysis of photography for starting design with glass model on (a) central field, and (b) edge of field.

At this stage, we began developing an interface for communication with a GPT-4 model, implemented as a Java application. The application is linked to the OpenAI model via API (Application Programming Interface) protocol [23].

In this context, a GPT-4 was trained to write macros based on specified parameters and save them as ready-to-use files for activating the global search algorithm within the Synopsys OSD software. Several macros with different operand values for illumination, which proved effective, were utilized as the training examples.

In addition, to train an OpenAI model about useful starting points, we used nine training sets of images as outputs from nine different global search runs (90 starting designs). Once trained, the framework based on a GPT-4 model can analyze the shapes of smartphone lenses it has not previously encountered and classify them based on ray tracing and lens arrangement.

Please note one remarkable outcome of the study: using only the provided image layouts of 10 designs, the GPT-4 selected the

same two best starting designs as the global search algorithm, which was based on layout and transverse aberration. To emphasize, this result was achieved without prior supervised training and before any specific requirements related to the design of smartphone optics were provided. Table 2 presents the outputs of the GPT-4 based on the provided image, using the starting designs from Fig. 5.

The front-end application based on the OpenAI model, featuring options for macro creation, evaluation of starting designs and interaction with the GPT-4 model, is shown in Fig. 8.

Figure 8 shows the app interface for the OpenAI model. The interface is titled "Artificial Intelligence Assistance" and includes the following sections:

- Please specify the parameters of the smartphone lens:**
 - Lens Specifications:** Enter FN, FOV/2, DN/2, Image Height, Focal Length, Number of Lenses, Illumination, Glass Material (comma separated)
 - Merit Function:** Enter Aspheric Order
- Enter Text for ChatGPT:** Enter your query for ChatGPT
- Enter Training Password:** Enter 'password' for training
- Send to ChatGPT:** Generate Lens Macro
- Upload Design for Evaluation:** Choose File No file chosen

Fig. 8. App Interface for the OpenAI model.

Table2. Design evaluation based on the GPT-4 model

GPT-4 without training on design task	GPT-4 with supervised training
<p>Best Design:</p> <p>If minimizing spot size and optical aberrations is critical:</p> <ul style="list-style-type: none"> • Top-Left and Bottom-Left systems are superior. <p>If wide-angle imaging or light gathering is the priority:</p> <ul style="list-style-type: none"> • Top-Right or Bottom-Right 	<p>Final Recommendation:</p> <p>If Compactness and Transverse Aberration Correction Are Key:</p> <p>The Top-Left Design is better because:</p> <p>It achieves sharper edge performance despite its slightly less balanced field correction. Its compactness makes it easier to fit into slim smartphone designs.</p> <p>If Wide-Angle Performance and Balanced Aberration Correction Are Key:</p> <p>The Bottom-Left Design is better because:</p> <p>It uses the ideal convex-concave-convex-concave arrangement.</p> <p>It provides more consistent sharpness and distortion control across the image field, which is essential for wide-angle smartphone lenses.</p>

We have introduced restrictions for commands longer than six characters but allowed the option to send text and longer commands from the app using a password. This way, we have introduced authorization for developers to send training commands to the GPT-4 in order to prevent misleading data. Lens specifications must follow a particular format, such as FN2.5, FV40, DN1, IH4, IL45.5, etc (see Application of GPT-4).

At this stage of the project, we have successfully developed an application for generating and evaluating starting designs using the OpenAI model. In this respect, proposed methodology enables the generation of starting designs for high-resolution smartphone lens within a less than 5 minutes using just a single input text to an OpenAI application to create macro and one click to run global search.

3. OPTIMIZATION OF STARTING DESIGN WITH RULE-BASED AI ALGORITHMS

The optimization of smartphone lenses is crucial for achieving high-quality pixels and ultra-sharp resolutions, with modern smartphones now exceeding incredible 200 megapixels in flagship models.

One effective and common technique to optimize the image quality of smartphone lenses is by utilizing aspherical surfaces. This involves increasing the number of higher-order aspherical surfaces by introducing coefficients of high-order aspherics through simultaneous local optimization.

Another effective solution is to insert an additional refractive element into the optical system. This can be done using the automatic element insertion (AEI) feature, which is based on a Saddle Point Build algorithm [24][25].

In this design task we performed local optimization using rule-based AI algorithms for automatic aspherical assignment (AAA) and automatic replacement of glass (ARG).

To incorporate aspherics onto all lens surfaces, we gradually introduced aspheric coefficients into the merit function, monitoring RMS spot size, distortion, and illumination [26].

Outlined below are the lines of the merit function macro that we used to assign 4 aspherical coefficients of 10th order to the first four optical surfaces.

VY 1 G 10

VY 2 G 10

VY 3 G 10

VY 4 G 10

With such requests, we introduce four more parameters in further optimization of starting point in Fig 3.

Next, we assign aspherical coefficients to next four optical surfaces from 5 to 8. Following this principle, we performed gradually and steady optimization between local minima of optical system. The optimization performed using the applied merit function (see supplement 1) indicated that time consumption was highly dependent on the number of optimization cycles and the complexity of the aspherics.

Due to the higher-order aspherics, we recommend reducing the number of optimization cycles when introducing new coefficient terms. It is essential to correct optical aberrations by monitoring the RMS spot size under strict constraints on both illumination and distortion.

To introduce an additional four aspheric coefficients on all surfaces, the optimization using the merit function was repeated four times for the first two lenses and four times for the second two lenses closer to the image plane. It should be emphasized that only radially symmetric aspheric coefficients were utilized. However, after incorporating 19th-order aspherics on all surfaces of the initial design, we did not achieve satisfactory MTF and lateral color performance.

In the next step, we employed the AEI (Automatic Element Insertion) algorithm, requiring the insertion of an additional lens into the starting design shown in Fig. 3, within the space between the 4th and 8th optical surfaces. After determining the optimal position for the new element, the algorithm inserted a fourth lens with the same material as the lens behind it (ZEON480R). A 19th-order aspherical surface was also added to both optical surfaces of the inserted lens through repeated optimization. **Fig. 9** illustrates the optimized starting point of a smartphone lens with aspherical lenses of higher 19th order.

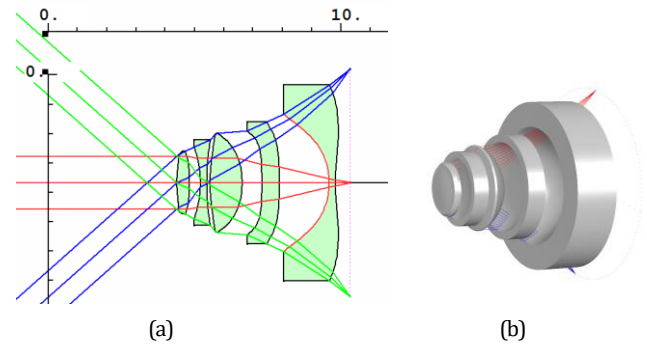


Fig. 9 Final design of smartphone optics with two plastic materials for 21.4 megapixel (a) 2D (b) 3D image.

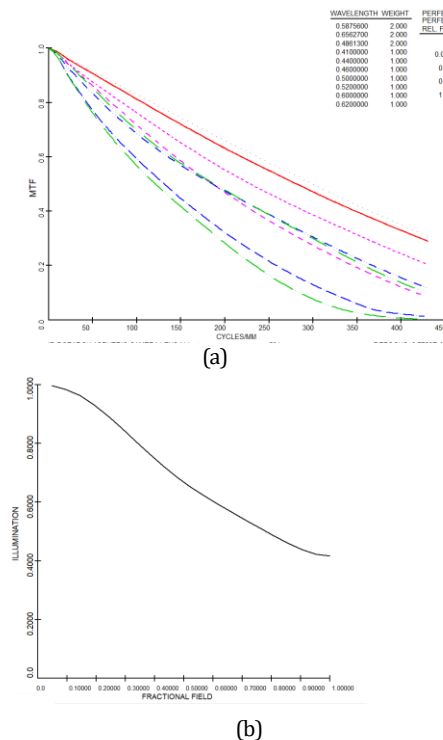


Fig. 10. Assessment of smartphone lens with two plastic materials: a) multi-field modulation transfer function b) relative illumination over field of view.

Lateral color remains below 2 micrometers at the edge of the field of view. In Fig. 10 (a) MTF analysis shows acceptable requirements for image quality of smartphone lens [27]. The MTF of the central field at half the Nyquist frequency is greater than 0.5,

and the full field of view is greater than 0.25. MTF at the spatial frequency of 446 lp/mm is close to zero and could be optimized for better minima. A distortion is below 3 %. The relative illumination is greater than 42 percent and is shown in Fig. 10b).

In Fig. 11, the image quality at the edge of the field at 0.9 FOV and in the central field is satisfactory. The sharpness and resolution at the edges of the field are comparable to those in the central region, meeting the requirements for imaging. The RMS spot is less than 2 micrometers in the central field and middle of the FOV, while at the edge of the field, it is greater than 4 micrometers and could still be optimized with further aspheric introduction. We decided not to introduce more than the 19th-order aspherics into this design, so the introduction of all new aspheric surface coefficients takes around 20 minutes. At this stage, the GPT-4 model was trained to write a merit function macro containing operands for aspheric surfaces, aiding further optimization.

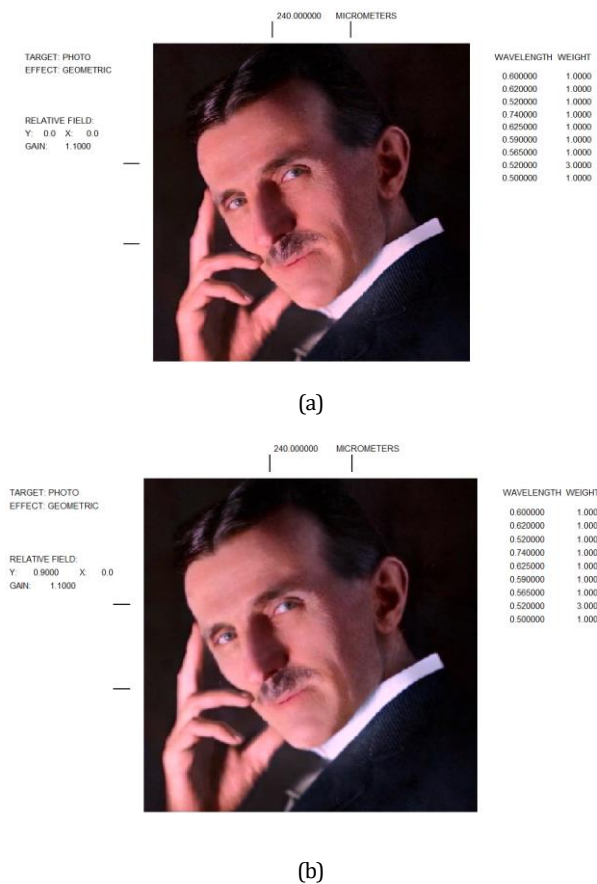


Fig. 11. Imaging quality analysis of photography for designed smartphone optics with two plastic materials on (a) central field (b) edge of field.

More specifically, we fine-tuned a GPT-4 model to edit and add aspheric coefficients to the merit function based on input to the application. In either case, what would traditionally need to be done manually to adjust the coefficients of aspherics in a matter of minutes, an OpenAI model assists by creating a macro for the merit function in seconds.

Regarding the second starting design with glass model shown in Fig. 5 (upper left), we utilized Automatic Replacement Glass (ARG)

feature to substitute the glass model with a plastic material. Previously, we constrained the material index region to plastic materials within the macro during the global search of starting design. Additional command lines in the merit function macro enabled the replacement of the glass model with plastic materials from the unusual glass catalog:

ARGLASS 3 QUIET ! Start of ARGLASS input.

CAT U ! Specify the Unusual glass catalog.

INCLUDE 1 TO 8 ! Surfaces from 1 to 8.

PREF ! Only preferred glass materials

GO

The cover glass was previously determined in the macro for the global search using BK7 material index. The ARG algorithm successfully identified three suitable plastic materials within one minute of optimization. After substituting the glass model, we proceeded with the design optimization by introducing additional aspheric coefficients to all surfaces of the plastic lenses.

To further improve image performance, we introduced 18th-order aspherics on the first two lenses and 21st-order aspherics on the third and fourth lenses. This involved repeated optimization using a merit function that varied in terms of the aspheric coefficients.

Shortcoming of our optimization methodology is following:

- 1) we ask an OpenAI model to add 4 new aspheric coefficients to the merit function,
- 2) open the file of the new merit function created by the OpenAI model in SYNOPSIS, and perform optimization,
- 3) repeat the first two steps for new aspheric coefficients.

In principle, it can take no more than 30 minutes, considering a well-adjusted, logical, and effective optimization cycle length. It should be emphasized that the core design strategy is based on minimizing the effort of the optical designer and additional analytics grounded in experience and talent.

The final design, incorporating 21st-order aspheric coefficients on the third and fourth lenses, is shown in Fig. 12 in both 2D and 3D views. The size of the designed smartphone lens, illustrated in Fig. 12 (a) is displayed using a coordinate system in millimeters. Lens data of designed photo-objectives can be seen in supplement 1.

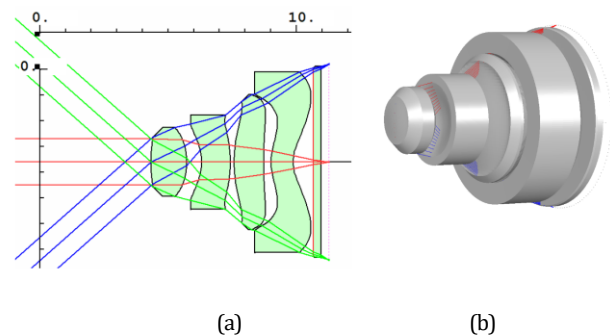


Fig. 12. Final design of smartphone lens with three plastic materials and cover glass for 21.4 megapixel (a) 2D (b) 3D image.

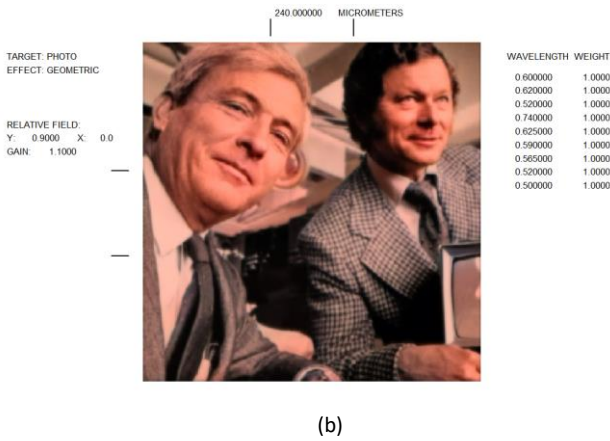
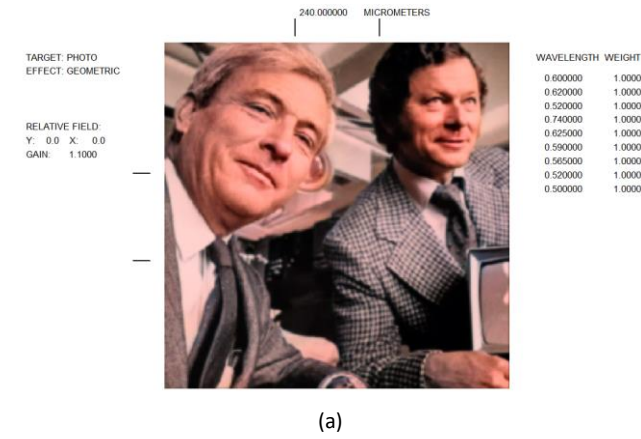


Fig. 13. Imaging quality analysis of photography on (a) central field (b) edge of field.

Illumination has been enhanced to exceed 49%, compared to the initial design of 38%. An analysis of image quality for photography is shown in Fig. 13. The resolution achieved is satisfactory in both the central region and the field edges. To illustrate a more colorful environment, an analysis of the quality of a segment of the panoramic photography is presented in Fig.14.

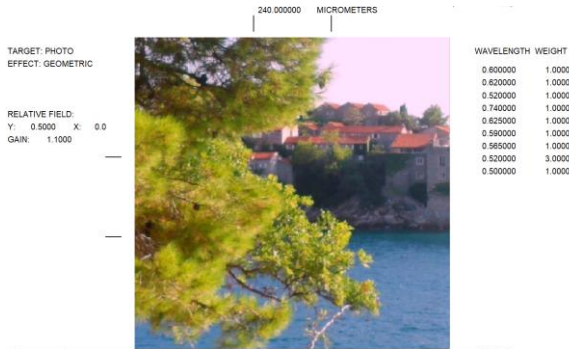


Fig. 14. Imaging quality analysis of colorful environment on half of field.

In this case, we introduced more complex aspheric surfaces with eight coefficients, compensating for the need for an additional lens, which could be considered in future optimization.

The multifield MTF is optimized at a spatial frequency of 446 lp/mm, where the full field exceeds 0.05, as shown in Figure 15. The central FOV exceeds 0.2 at the limit frequency and is greater than 0.5 at half the spatial frequency (223 lp/mm), meeting common requirements for smartphone optics. The MTF value at the field edges is slightly lower, with room for further optimization.

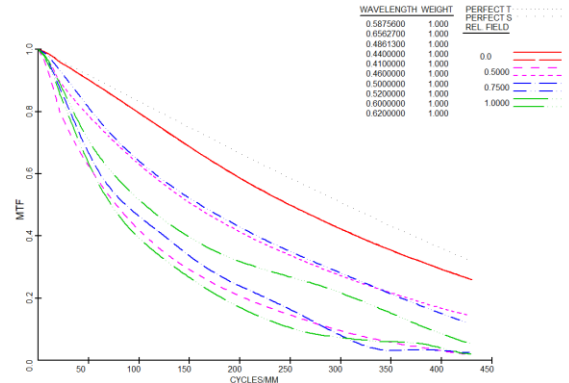
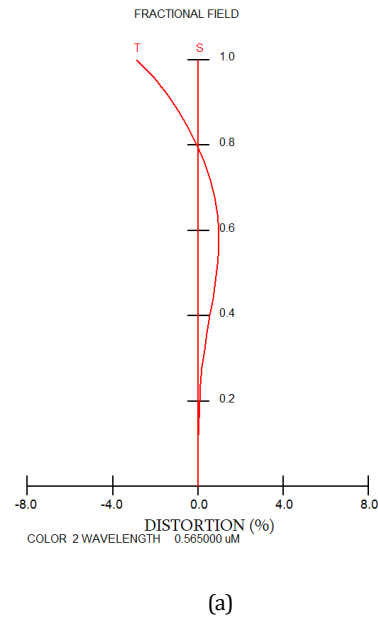


Fig. 15. Multifield modulation transfer function of smartphone lens with three plastic materials and cover glass.

The RMS spot size across the entire field is less than 3 micrometers, and lateral color is controlled within 1.4 micrometers. Distortion is below 4 % at the field edge, and relative illumination curve is larger than 49 % over FOV, as shown in Fig. 16.

The GPT-4 framework is trained to identify this layout with 4 lenses as the most successful smartphone lens design, achieved in this environment, delivering a resolution of 21.4 megapixels.



(a)

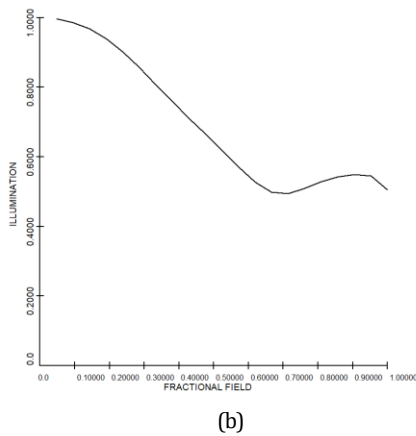


Fig. 16. (a) Distortion of designed smartphone lens (b) relative illumination over field of view.

4. CONCLUSION

In this paper, we present findings and insights from a study on design methodology of smartphone optics by combining generative and rule-based AI algorithms. The innovative approach utilizes the GPT-4 module to generate macros for global optimization algorithms, enhancing the efficiency of designing smartphone lenses.

A comprehensive global search for optimal starting points was conducted, yielding reliable training sets essential for fine-tuned model of OpenAI. In this context, generative artificial intelligence – the GPT-4 was trained to write macros based on specified parameters and save them as ready-to-use files for activating the global search algorithm within the Synopsys OSD software. Utilizing generated starting designs, the GPT-4 model is trained to evaluate the performance of optical layouts by analyzing lens configurations and ray tracing principles. In addition, the GPT-4 was trained to generate a merit function macro containing operands for aspheric surfaces and insertion of lens, aiding further optimization.

In this way, we trained generative AI to use rule-based AI algorithms in the merit function based on requirements. Combining principles and computing power of different algorithms, we developed a front-end application featuring options for macro creation, evaluation of starting designs, and interaction with the OpenAI model. Through this, we designed two 21.4-megapixel smartphone lenses from different starting points, demonstrating the practical value of the proposed design methodology in achieving high-performance smartphone optics. With this paper we encourage vendors of lens design software to implement more advanced features with application of AI, as it could significantly enhance design flexibility and innovation in optical design.

The proposed methodology is versatile and can be expanded to design and evaluation of various optical systems employing synergy of different algorithms.

Funding. European Union.

Acknowledgments.

Disclosures. The authors declare no conflicts of interest.

Supplemental document. See Supplement 1 for supporting content.

Data availability. Data underlying the results presented in this paper are not publicly available at this time but may be obtained from the authors upon reasonable request.

References

1. P. Wang, "On defining artificial intelligence," *J. Artif. Gen. Intell.* **10**, 1–37 (2019).
2. G. Wetzstein, A. Ozcan, and S. Gigan, "Inference in artificial intelligence with deep optics and photonics," *Nature* **588**, 39–47 (2020).
3. M. S. S. Rahman and A. Ozcan, "Physics and artificial intelligence: illuminating the future of optics and photonics," *Adv. Photon.* **6**(5), 050500 (2024).
4. C. Rodríguez, S. Arlt, and L. Möckl, "Automated discovery of experimental designs in super-resolution microscopy with XLuminA," *Nat. Commun.* **15**, 10658 (2024).
5. K. Yadav, S. Bidnyk, and A. Balakrishnan, "Artificial intelligence and machine learning in optics: tutorial," *J. Opt. Soc. Am. B* **41**, 1739-1753 (2024).
6. Norman and Bella, "Embrace the future," *Norman and Bella*, [Online]. Available: <https://normanandbella.com/embrace-the-future/>, accessed Feb. 10, 2025.
7. AIM Research, "How Nike is using AI to transform product design, customer experience, and operational efficiency," *AIM Research*, [Online]. Available: <https://aimresearch.co/uncategorized/how-nike-is-using-ai-to-transform-product-design-customer-experience-and-operational-efficiency>, accessed Feb. 10, 2025.
8. G. Côté, J. F. Lalonde, and S. Thibault, "Extrapolating from lens design databases using deep learning," *Opt. Express* **27**, 28279-28292 (2019).
9. T. Yang, D. Cheng, and Y. Wang, "Direct generation of starting points for freeform off-axis three-mirror imaging system design using neural network-based deep learning," *Opt. Express* **27**, 17228-17238 (2019).
10. Y. Nie, J. Zhang, R. Su, and H. Ottevaere, "Freeform optical system design with differentiable three-dimensional ray tracing and unsupervised learning," *Opt. Express* **31**, 7450-7465 (2023).
11. E. Tseng, A. Mosleh, F. Mannan, K. St-Arnaud, A. Sharma, Y. Peng, A. Braun, D. Nowrouzezahrai, J. Lalonde, and F. Heide, "Differentiable compound optics and processing pipeline optimization for end-to-end camera design," *ACM Trans. Graph.* **40**(2), 18 (2021).
12. D. C. Dilworth, "Applications of artificial intelligence to computer-aided lens design," *Proc. SPIE* **0766**, *Recent Trends in Optical Systems Design and Computer Lens Design Workshop*, 10 June 1987.
13. S. Thibault, G. Côté, J. Buque, and J. F. Lalonde, "Optical design at the age of AI," *EPJ Web Conf.* **266**, 03023 (2022).
14. I. Livshits and N. Zoric, "A concept of ultraviolet lithography system and design of its rear part using artificial intelligence for starting design," in *Proceedings of the 4th Int. Conf. on Photonics, Optics and Laser Technology (PHOTOPTICS)*, Rome, Italy, pp. 1-5 (2016).
15. X. Yang, Q. Fu, and W. Heidrich, "Curriculum learning for ab initio deep learned refractive optics," *Nat. Commun.* **15**, 6572 (2024).

16. X. Wu and Y. Wang, "Design of 21 mega-pixel mobile phone lens," *Proc. SPIE* **12757**, 3rd Int. Conf. on Laser, Optics, and Optoelectronic Technology (LOPET 2023), 127571V (2023).
17. T. Steinich and V. Blahnik, "Optical design of camera optics for mobile phones," *Adv. Opt. Technol.* **1**(1-2), 51-58 (2012).
18. Y. Yan and J. Sasian, "Miniature camera lens design with a freeform surface," in *Optical Design and Fabrication 2017 (Freeform, IODC, OFT)*, OSA Technical Digest (online) (Optica Publishing Group, 2017), paper JTU3A.3.
19. W. S. Boyle and G. E. Smith, "Charge coupled semiconductor devices," *Bell Syst. Tech. J.* **49**(4), 587–593 (1970).
20. T. Seger, C. Menke, M. Sonntag, and K. Urban, "Efficient evaluation of the Jacobian in the damped least-squares method for optical design problems using algorithmic differentiation," *Opt. Express* **33**, 3054-3067 (2025).
21. M.-A. Burcklen, H. Sauer, F. Diaz, and F. Goudail, "Joint digital-optical design of complex lenses using a surrogate image quality criterion adapted to commercial optical design software," *Appl. Opt.* **57**, 9005-9015 (2018)
22. N. Zoric, Y. Nie, S. Thibault, R. Prodanovic, and L. Thomas, "Global search algorithms in an automated design of starting points for a deep-UV lithography objective," *Appl. Opt.* **63**, 6960-6968 (2024).
23. T. Auger, E. Saroyan, "Overview of the OpenAI APIs. In: Generative AI for Web Development," Apress, Berkeley, CA.(2024).
https://doi.org/10.1007/979-8-8688-0885-2_6
24. D. Dilworth, "The ascendancy of numerical methods in lens design," *J. Imaging* **137** (2018).
25. Z. Hou, M. Nikolic, P. Benitez, and F. Bociort, "SMS2D designs as starting points for lens optimization," *Opt. Express* **26**, 32463–32474 (2018).
26. M. M. Rusinov, "Composition of Optical Systems," *Mashinostroenie Publ.*, 383 (1989).
27. R. Kingslake and R. B. Johnson, "Lens Design Fundamentals," Academic Press, Bellingham, WA, USA.